

## NATURE INSPIRED SYNTHESIS, PHYSICO-CHEMICAL CHARACTERIZATION OF Zn DOPED $\text{Fe}_3\text{O}_4$ NANOPARTICLES USING *ANDROGRAPHIS PANICULATA* (BURM. F.) NEES LEAF EXTRACT AND ASSESSMENT OF *IN VITRO* PANCREATIC ALPHA AMYLASE INHIBITORY ACTIVITY

A. S. SAKTHI ATHITHAN<sup>1</sup>, J. JEYASUNDARI<sup>2\*</sup>, D. RENUGA<sup>3</sup>, A. NAVEENA<sup>4</sup>

<sup>1,2,4</sup>Department of Chemistry, NMSSVN College/M. K University, Madurai 625019, Tamilnadu, India, <sup>3</sup>PG, Department of Chemistry, Sri Meenakshi College for Women/M. K University, Madurai 625002, Tamilnadu, India  
Email: jjsundariresearch16@gmail.com

Received: 31 Jul 2020, Revised and Accepted: 26 Sep 2020

### ABSTRACT

**Objective:** Magnetite ( $\text{Fe}_3\text{O}_4$ ) nanoparticles (NPs) have gained considerable attention in the Biomedical field. Evolution of new magnetic material based on the transition metal-doped magnetite has become the subject of increasing research interest. The main aim of the current investigation was to improve the diabetic potential, optical, magnetic, structural properties of magnetite nanoparticles and hence  $\text{Fe}_3\text{O}_4$  NPs were doped with a divalent transition element such as Zinc.

**Methods:** Zinc doped magnetite nanoparticles ( $\text{Zn-Fe}_3\text{O}_4$  NPs) were obtained through Co-precipitation methods using aqueous plant extract of *Andrographis paniculata* acted as an efficient stabilizer and a reducing agent. The structure, morphology, crystalline, optical and magnetic property of synthesized  $\text{Zn-Fe}_3\text{O}_4$  NPs were evaluated by X-ray diffraction (XRD), Scanning electron microscopy with Energy dispersive x-ray spectroscopy (SEM-EDX), Fourier transform infrared spectroscopy (FTIR), Ultraviolet-Visible (UV-Vis) Spectrophotometer and Vibrating scanning magnetometer (VSM).

**Results:** In XRD analysis, the average crystallite size of the synthesized  $\text{Zn-Fe}_3\text{O}_4$  NPs was found to be 5 nm exhibiting super paramagnetic behavior, which composes it an appealing possibility for biomedicines. The  $\text{Zn-Fe}_3\text{O}_4$  NPs had strongly inhibited the alpha ( $\alpha$ )-amylase enzyme and had proved their therapeutic role.

**Conclusion:** In conclusion,  $\text{Zn-Fe}_3\text{O}_4$  NPs is an excellent anti-diabetic agent to control type 2 diabetes mellitus.

**Keywords:** Alpha-amylase, *Andrographis paniculata*, SEM-EDX, VSM,  $\text{Zn-Fe}_3\text{O}_4$  NPs

© 2020 The Authors. Published by Innovare Academic Sciences Pvt Ltd. This is an open access article under the CC BY license (<http://creativecommons.org/licenses/by/4.0/>)  
DOI: <http://dx.doi.org/10.22159/ijap.2020v12i6.39278>. Journal homepage: <https://innovareacademics.in/journals/index.php/ijap>

### INTRODUCTION

Iron oxide nanoparticles (IONPs) are widely used in bioremediation systems because of their cost efficiency, magnetic strength, biocompatibility, easy water separation and surface modifiability. Maghemite ( $\gamma\text{-Fe}_2\text{O}_3$ ), Magnetite ( $\text{Fe}_3\text{O}_4$ ) and hematite ( $\alpha\text{-Fe}_2\text{O}_3$ ) are the most common IONPs found in nature [1]. Among these, Magnetite ( $\text{Fe}_3\text{O}_4$ ) is the strongest magnetic mineral on earth [2].  $\text{Fe}_3\text{O}_4$  NPs (magnetite nanoparticles) have a property that is ferromagnetic at RT (Room temperature) [3]. However, the magnetic behavior of magnetite nanoparticles depends largely on the preparation methods. In addition, the crystallite size and then surface morphology of  $\text{Fe}_3\text{O}_4$  crystal play a crucial role, which influences the magnetic properties of  $\text{Fe}_3\text{O}_4$  NPs [4, 5].

$\text{Fe}_3\text{O}_4$  consists of  $\text{Fe}^{2+}$  and  $\text{Fe}^{3+}$  in particular spinel format.  $\text{Fe}^{2+}$  species resides at octahedral sites and  $\text{Fe}^{3+}$  species are distributed between octahedral as well as tetrahedral sites. Structural  $\text{Fe}^{2+}$  ion in  $\text{Fe}_3\text{O}_4$  plays a major role part as an electron donor to start the reduction process [6]. Structural  $\text{Fe}^{2+}$  inserts  $\text{Fe}_3\text{O}_4$  with reducibility besides environmental contaminants. Even though  $\text{Fe}_3\text{O}_4$  stoichiometry ratio ( $\text{Fe}^{3+}/\text{Fe}^{2+}$ ) becomes lesser at the time of the reduction, the proximity of an active reducer, i.e., aqueous  $\text{Fe}^{2+}$ , can efficaciously recharge  $\text{Fe}_3\text{O}_4$  [7] and recuperate its reducibility. Due to its non-toxicity, Magnetite nanoparticles have attracted considerable interest in various applications [8].

After many research works, it has been proved that the IONPs concert can be improved further by doping. The synthesis of magnetite in the presence of divalent and trivalent cations of transition metals ( $\text{Zn}^{2+}$ ,  $\text{Mn}^{2+}$ ,  $\text{Co}^{2+}$ ,  $\text{Ni}^{2+}$ ,  $\text{Li}^{2+}$ ) can modify structural, optical, electrical, magnetic, saturation magnetization properties of iron oxide [9]. In an anoxic nature,  $\text{Zn}^{2+}$  can be accessed into the  $\text{Fe}_3\text{O}_4$  structure by the reduction of  $\text{Fe}^{3+}$  compounds with reducible iron bacteria, e. g., *Clostridium sp* and *Geobacter sulfurreducens*. The magnetic moment of  $\text{Fe}_3\text{O}_4$  increases with the addition of a small amount of Zinc, but decreases dramatically with

an increase in Zinc content, whichever is related to conversion in cation site order. At low Zinc level, tetrahedral site  $\text{Fe}^{3+}$  species is replaced by  $\text{Zn}^{2+}$  species, which is coupled with the oxidation of octahedral site  $\text{Fe}^{2+}$  to  $\text{Fe}^{3+}$  state. Thus, it controls the spinel structure as well as it also enhances the magnetic property by bettering the  $\text{Fe}^{2+}$ - $\text{Fe}^{3+}$  species interaction [10].

*Andrographis paniculata* (AP) (Burm. f.) Nees has been used to cure a wide range of biomedical applications, including hepatitis, sexual dysfunctions, anti-diarrheal, anti-hyperglycemic, anti-malarial, antioxidant, cardiovascular, inflammatory activity, microbial activity, cancer activity, hepatoprotective, anti-HIV and immunostimulatory [11]. After a detailed literature study, it has been found that the preparation of nanoparticles by using *Andrographis paniculata* (plant) has not been attempted yet by any researcher.

The principle of this study was to improve its diabetic potentiality of  $\text{Fe}_3\text{O}_4$  NPs; we report here synthesis and characterization of  $\text{Zn-Fe}_3\text{O}_4$  NPs by using *Andrographis paniculata* leaf extract without any stabilizers, distributors and oxidants. The obtained zinc doped magnetic nanoparticles ( $\text{Zn-Fe}_3\text{O}_4$  NPs) were characterized using physicochemical techniques such as UV-Vis, VSM, FTIR, SEM, XRD and EDX, respectively. The synthesized  $\text{Zn-Fe}_3\text{O}_4$  NPs were evaluated for their antidiabetic potential by alpha-amylase inhibitory activity.

### MATERIALS AND METHODS

#### Materials

The chemicals required were purchased from the following sources: Iron sulphate, Zinc chloride, Iron chloride and ammonium hydroxide ( $\text{NH}_4\text{OH}$ ) from Sigma-Aldrich with 99% purity.

#### Preparation of AP extract

Indian medicinal herb, *Andrographis paniculata* (Burm. f.) Nees leaves were collected from local area of Nagercoil in the month of March and botanical identity was confirmed by Dr. Mahesh,

Assistant professor, Department of botany, ST. Hindu College, Nagercoil. The Voucher specimen number of *Andrographis paniculata* (STHCH10) was deposited in the institute for future reference. The fresh leaves were first cleaned with tap water followed by de-ionized (DI) water to remove adhering soil and unwanted dust particles, cut into fine pieces and dried out at RT.

Approximately 12g of the leaves were weighed separately and shifted into 400 ml beaker containing 150 ml of DI water and heated for 25 min, followed by filtering through Whatman filter paper to remove biomaterials. Finally, *Andrographis paniculata* extract was stored at 4 °C in Erlenmeyer flasks for the preparation of Zn-Fe<sub>3</sub>O<sub>4</sub> Nps [12].

### Phytochemical screening

Fresh and healthy leaves were selected for phytochemical analysis. The phytochemical screening of *Andrographis paniculata* was carried out by the standard method that was previously discussed [13].

### Synthesis of Zn-Fe<sub>3</sub>O<sub>4</sub> nanoparticles

Zinc doped magnetite nanoparticles were carried out by an improved co-precipitation method. The standard stock solutions of FeCl<sub>3</sub>·7H<sub>2</sub>O, FeSO<sub>4</sub>·7H<sub>2</sub>O and ZnCl<sub>2</sub>·6H<sub>2</sub>O were added in the ratio of 2: 1: 0.2. This solution was heated and maintained at 35-45 °C under a mild stirring using a magnetic stirrer for 20 min. After 10 min, *Andrographis paniculata* extract was added slowly into the solution. After 1 h, 1N ammonium hydroxide was added into the solution drop by drop for uniform precipitation of zinc doped magnetite nanoparticles. The final P<sup>H</sup> of the mixture solution was reached to 11.

The mixture solution was left undisturbed and allowed to settle down at room temperature. The black coloured Zn-Fe<sub>3</sub>O<sub>4</sub> NPs got deposited at the base of the conical flask. The deposited nanoparticles were repeatedly washed with DI water.

Then the solution is centrifuged at 6000 rpm and the colloidal solution is retained. The colloidal solution acquired is then transferred to the Petri plate and dried in a dryer oven machine at 150 °C for 10 h. The dried sample is again calcinated using a muffle furnace [14]. The resulting nanoparticles are subjected to characterization and application (fig. 1).

### In vitro pancreatic alpha-amylase inhibitory assay

The inhibitory activity of zinc doped magnetite nanoparticles against the alpha-amylase enzyme was studied, according to previous resources [15]. Acarbose is a standard pharmacological drug to cure type-II diabetes mellitus. The positive control was to be used as a pharmacological drug (pharmacological inhibitor).

### Characterization methods

The phase purity and crystalline structure of the prepared nanoparticles were investigated with an XRD machine (PANalytical, Philips PW 1830) using CuKα radiation in the 2 Theta ranges from 10°-80°. SEM attached with EDX were done using Quanta FEG 250 instrument; while electronic and FT-IR spectra were investigated using Shimadzu model (UV-1800) and Perkin Elmer model (version 10,300) FTIR spectrometer, respectively. Magnetic behavior of the Zn-Fe<sub>3</sub>O<sub>4</sub>NPs was examined using a vibrational sample magnetometer (VSM, Cryogenic, UK).

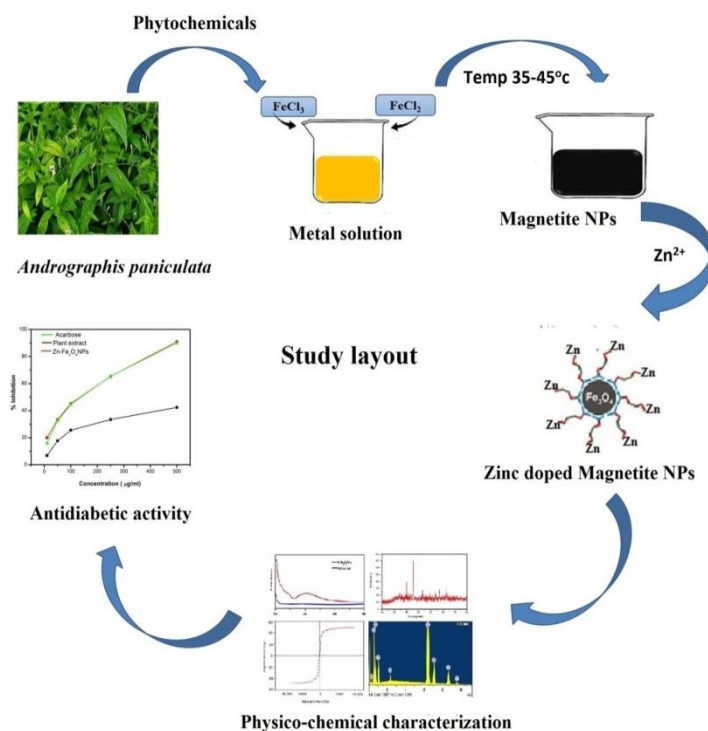


Fig. 1: Schematic diagram of synthesized zinc doped magnetite NPs

## RESULTS AND DISCUSSION

### Phytochemical screening for AP extract

The leaf extract of *Andrographis paniculata* was analyzed by phytochemical screening for the evaluation of bioactive compounds. Ten phytochemical tests were tested, out of which seven were confirmed (table 1) in the *Andrographis paniculata* (AP) extract.

The bioactive compounds detected in the leaf extract act as a reducer and stabilizer in the nanoparticle synthesis, which includes

alkaloids, flavonoids, terpenoids, saponins, phlobatannins, tannins and phenols, respectively [16]. The aqueous *Andrographis paniculata* leaf extract was found to have these constituents, suggesting that they are the excellent starting material for synthesizing zinc doped magnetite nanoparticles.

### UV-Vis absorption spectra

The stability as well as the formation of Zn-Fe<sub>3</sub>O<sub>4</sub> NPs in colloidal suspension, is examined by using UV-Visible spectroscopy. Extinction spectra of *Andrographis paniculata* and synthesized Zn-Fe<sub>3</sub>O<sub>4</sub> Nps are

depicted in fig. 2. The absorption peak was not observed in *Andrographis paniculata* extract and however, the green synthesized zinc doped magnetite nanoparticles reveals that a significant absorption peak was

observed at 380 nm resulting from the surface Plasmon resonance. The optical absorption maximum is found to be increased in doping Zn<sup>2+</sup> metal ion with bulk magnetite nanoparticles [17].

Table 1: Phytochemical analysis of *Andrographis paniculata* extract

Phytochemicals	Aqueous extract
Alkaloids	+
carbohydrates	-
Terpenoids	+
Cardiac glycosides	-
Phlobatannins	+
Tannins	+
glycoside	-
Saponins	+
flavonoids	+
phenols	+

Presence (+): Absence (-)

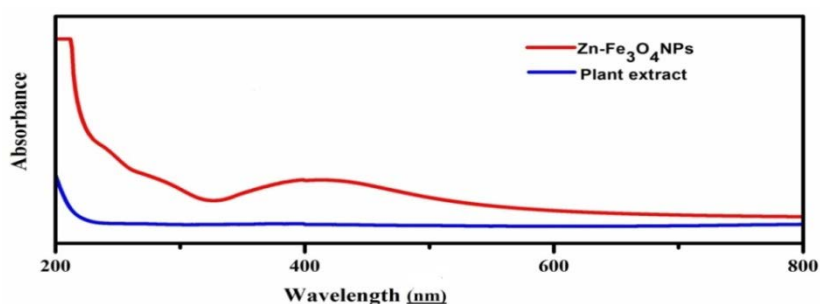


Fig. 2: Ultraviolet-visible absorption spectra of plant extract (AP) extract and Zn-Fe<sub>3</sub>O<sub>4</sub>NPs

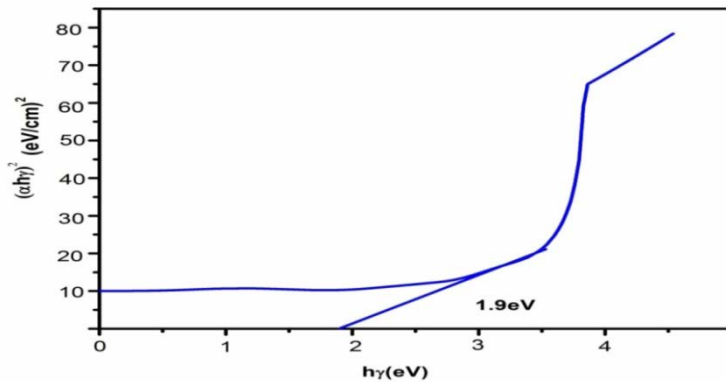


Fig. 3: Optical direct energy band gap detection of Zn-Fe<sub>3</sub>O<sub>4</sub>NPs

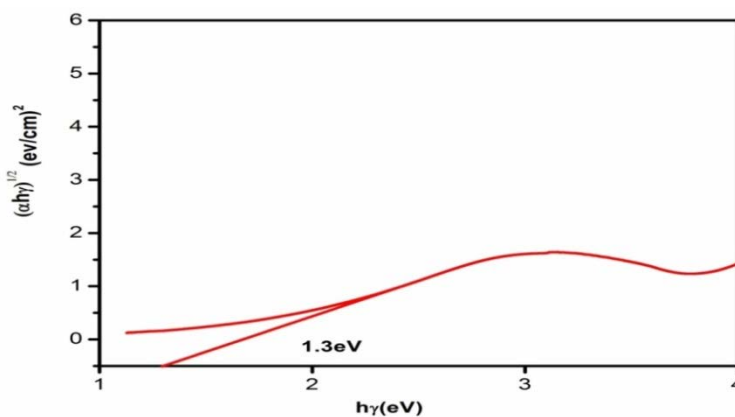


Fig. 4: Optical indirect energy band gap detection of Zn-Fe<sub>3</sub>O<sub>4</sub>NPs

### Band gap calculation

The energy band gap for the prepared nanoparticles is evaluated by Tauc relation

$$\alpha h\nu = I(h\nu - E_g)^2$$

Where  $\alpha$ ,  $I$ ,  $h$ ,  $\nu$  and  $E_g$  are linear absorption coefficient, proportionality constant, Planck's constant, photon frequency and optical energy band gap. The optical energy of the band gap can be evaluated by plotting  $(\alpha h\nu)^2$ ,  $(\alpha h\nu)^{1/2}$  and photon frequency will be made (fig. 3 and 4). The energy of band gap for Zn-Fe<sub>3</sub>O<sub>4</sub>Nps was found to be 1.9eV (direct band gap) and 1.3eV (indirect band gap), which is smaller than bulk Fe<sub>3</sub>O<sub>4</sub>NPs [18]. The outcome confirmed that zinc metal ion plays a significant role to reduce the energy band gap of the magnetite nanoparticles.

### FTIR spectral analysis

FTIR spectra were studied to analyze the bioactive functional groups of *Andrographis paniculata*, which acted as a reducer, capping and stabilizing agent in the preparation of Zn-Fe<sub>3</sub>O<sub>4</sub>Nps. The spectrum of the *Andrographis paniculata* indicated a high intense absorption peak at 3436,2071,1634,1119,666 cm<sup>-1</sup>, whereas the intense

absorption peaks of synthesized Zn-Fe<sub>3</sub>O<sub>4</sub>Nps were indicated at 3446, 2340, 1615,1111,616, 552 and 435 cm<sup>-1</sup>(fig. 5). The absorption band at 3446 cm<sup>-1</sup> in the *Andrographis paniculata* extract was attributed to the O-H stretches [19], while absorption peak at 1634 cm<sup>-1</sup> and 1119 cm<sup>-1</sup> were contributed to C=O stretches [20] and C-O-C stretches, respectively. All the bands were shifted, indicating the bioactive group involvement and interactions of NPs with the *Andrographis paniculata* extract, presence of bioactive compounds on the surface of Zn-Fe<sub>3</sub>O<sub>4</sub>Nps has an influence on the FTIR peaks. Two strong absorption peaks were found at 552 cm<sup>-1</sup> and 435 cm<sup>-1</sup> in the spectrum of synthesized nanoparticles, which is related to the Fe-O stretching vibration mode of magnetite (Fe<sub>3</sub>O<sub>4</sub>). The absorption peak at 552 cm<sup>-1</sup> can be contributed to the intrinsic stretching vibration of metal at the tetrahedral site, whereas the peak found at 435 cm<sup>-1</sup> is corresponds to octahedral stretches of Fe-O [21]. The weak absorption band at 616 cm<sup>-1</sup> is associated with Zn-O stretching vibration [22]. The above information confirms the formation of Zn-Fe<sub>3</sub>O<sub>4</sub>NPs. Based on FTIR, the bioactive compounds found in the *Andrographis paniculata* extract strongly suggested the conformation of alkaloids, terpenoids, flavonoids, saponins, phlorotannins, phenols and tannins. These bioactive compounds acted as a reducer and efficient stabilizing agent for Zn-Fe<sub>3</sub>O<sub>4</sub>NPs in the solution.

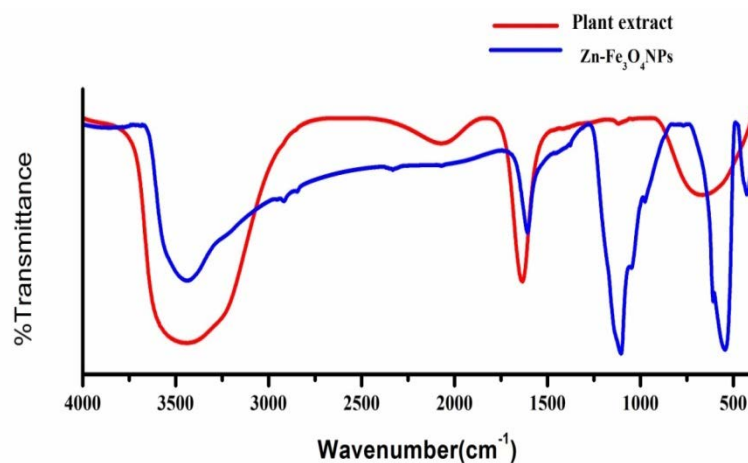


Fig. 5: FTIR spectra for the plant extract (AP) and Zn-Fe<sub>3</sub>O<sub>4</sub>NPs

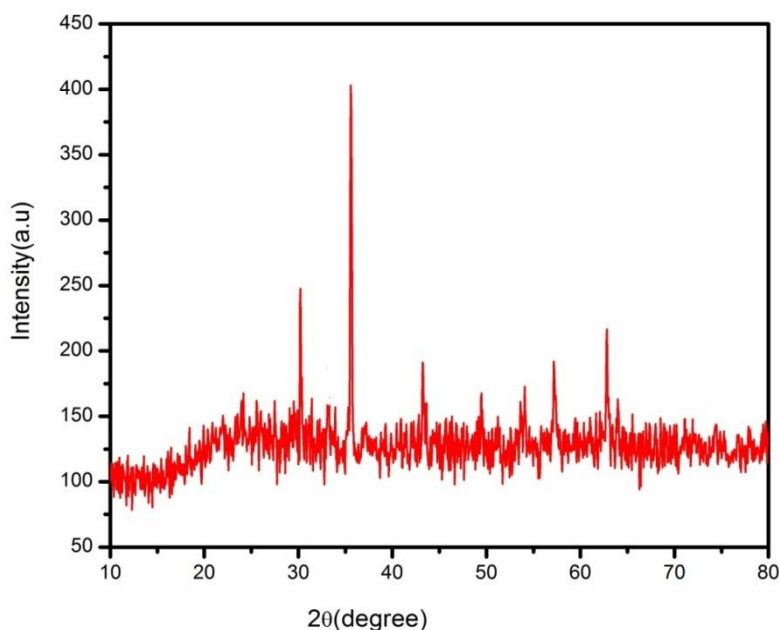


Fig. 6: XRD pattern of Zn-Fe<sub>3</sub>O<sub>4</sub>NPs synthesized using *Andrographis paniculata* extract

### XRD spectral studies

The crystalline size and structural identification of the material were detected by using powder XRD spectral studies. Fig. 6 demonstrates the XRD spectral data of Zn-Fe<sub>3</sub>O<sub>4</sub> NPs. The crystallite size of zinc doped magnetite nanoparticles can be evaluated using the Debye Scherrer equation; the required equation is

$$D = 0.9\lambda/\beta\cos\theta$$

The estimated size of the Zn-Fe<sub>3</sub>O<sub>4</sub> nanoparticles was calculated to be 5 nanometres, respectively. The synthesized material showed the major diffraction peaks for prepared crystalline nanoparticles at  $2\theta$  values of 30.27, 35.60, 43.23, 53.87, 57.23, 62.78 degrees corresponding to the crystal planes at (2 2 0), (311), (400), (422), (511), (440) respectively. All these diffraction peaks clearly coincide with the diffractions of iron oxide nanoparticles (magnetite phase). No other secondary phase is detected to prove the formation of other zinc-based structures such as simonkolleite, hydroxyzine, etc. So, we might conclude that Fe<sub>3</sub>O<sub>4</sub> NPs has been formed with high phase crystalline purity and Fe ions have successfully replaced by

zinc ions. Furthermore, this XRD spectral pattern is well-matched with early reported zinc metal-doped iron oxide nanoparticles [23]. The XRD spectral pattern is matched with pure cubic magnetite nanoparticles with the Joint Committee of Powder Diffraction Standards (JCPDS File no 01-074-1910).

### SEM-EDX analysis

The powder sample was analyzed for the morphological character of the Zinc doped magnetite nanoparticles by using SEM at different magnifications, including 2  $\mu$ m, 5  $\mu$ m and 10  $\mu$ m. The SEM images of zinc doped magnetite nanoparticles using *Andrographis paniculata* leaf extract are shown in fig. 7. SEM micrographs reveal that the surface morphology of the nanoparticles is cubic in shape [24]. The intense peak obtained from EDX spectra is Zn, Fe and O (fig. 8). The composition of zinc, iron and oxygen element is about 5.26, 35.71 and 52.18 % for Zn-Fe<sub>3</sub>O<sub>4</sub> NPs. EDX spectra also detect the presence of C and S, which may originate from the biomolecules present in the *Andrographis paniculata* extract. Therefore elemental studies confirm that the synthesized nanoparticles are pure without any impurity peaks.

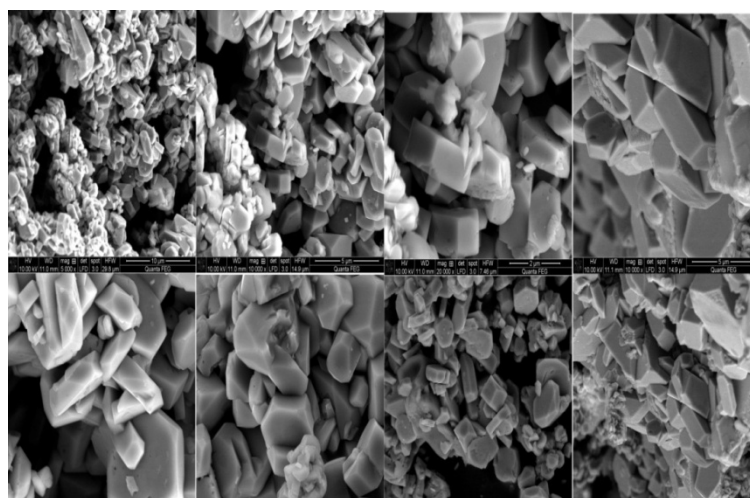


Fig. 7: SEM micrographs of the synthesized nanoparticles obtained through co-precipitation method using *Andrographis paniculata* extract, at different magnifications

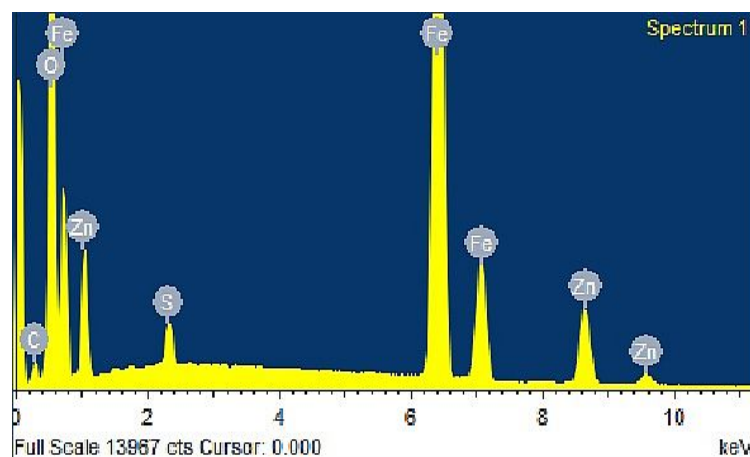


Fig. 8: EDX spectra of synthesized Zn-Fe<sub>3</sub>O<sub>4</sub>NPs

### VSM study

The magnetic behavior of zinc doped magnetite nanoparticles was evaluated by vibrating scanning magnetometer. The applied magnetic field was between -15,000 Oe to 15,000 Oe. The magnetization curve of the synthesized nanoparticles is depicted

in fig. 9. The measured magnetic saturation value of Zn-Fe<sub>3</sub>O<sub>4</sub> NPs is 70 emu/g at 300 K temperature, which is higher than that of bulk magnetite (Fe<sub>3</sub>O<sub>4</sub>) [25]. The obtained result reveals that the synthesized Zn-Fe<sub>3</sub>O<sub>4</sub> nanoparticles are super paramagnetic (particle size 5 nm) at room temperature.



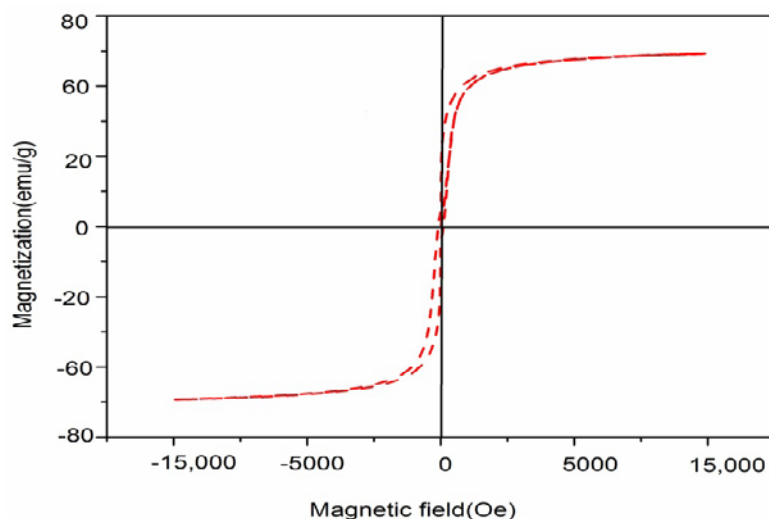


Fig. 9: Room temperature VSM spectra of for the synthesized Zn-Fe<sub>3</sub>O<sub>4</sub>NPs

### Antidiabetic activity

#### The inhibition activity of zinc doped magnetite nanoparticles against alpha-amylase

Diabetes mellitus is a major metabolic disease in which there are high blood sugar levels over an extended period. A medical approach to control hyperglycemia is to suppress the alpha-amylase enzyme. The carbohydrate digestive enzyme ( $\alpha$ -amylase) is used for the conversion of

carbohydrates into monosaccharides, which is the major reason for increasing of high blood sugar levels in the human body. Therefore, synthesizing compounds having strong inhibitory activities towards digestive enzymes is an easy route to cure diabetes [26]. The inhibitory activity of green synthesized Zn-Fe<sub>3</sub>O<sub>4</sub> NPs in combination with commercially used pharmacological inhibitor, Acarbose, was examined. The results indicate that the digestive enzyme was significantly inhibited with various concentrations of Zn-Fe<sub>3</sub>O<sub>4</sub> nanoparticles.

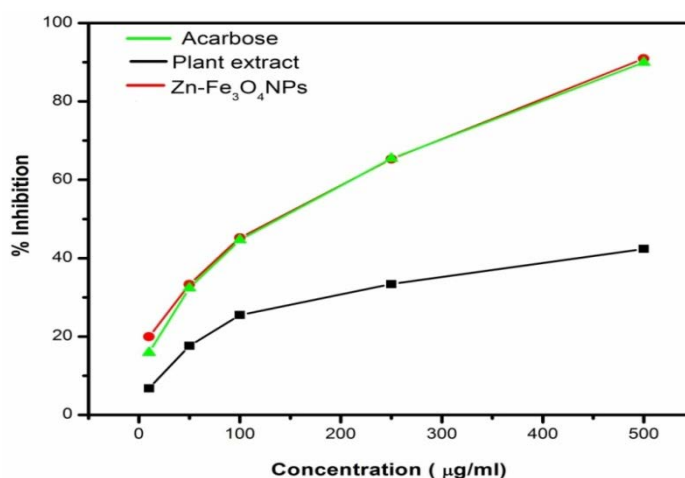


Fig. 10: Antidiabetic potential of synthesized Zn-Fe<sub>3</sub>O<sub>4</sub>NPs based on inhibition of alpha-amylase activity

Comparison of pancreatic alpha-amylase inhibition of plant extract (AP), Acarbose, and Zn-Fe<sub>3</sub>O<sub>4</sub> nanoparticles were shown in fig. 10. The percentage inhibition of zinc doped magnetite nanoparticles at various concentrations (10, 50, 100, 250 and 500) was found to be 19.93, 33.3, 45.2, 65.32, and 90.91 %, respectively. Hence the biomolecules present in the *Andrographis paniculata* extract likely improved the diabetic character of the synthesized nanoparticles [14]. Based on the results, blank < Acarbose < Zn-Fe<sub>3</sub>O<sub>4</sub> NPs inhibited the alpha-amylase enzyme and thus prevented the further hydrolysis of carbohydrates and controls the high blood sugar level in type-2 diabetes patients.

### CONCLUSION

The zinc doped magnetite nanoparticles were successfully obtained by using a simple, eco-friendly technique from the selected natural plant (*Andrographis paniculata*) extract. This study aims at

investigating Zn doping effects on optical, magnetic, and structural properties of magnetite nanoparticles. Based on the obtained results, Optical studies confirm that band gap energy decreases while doping with a transition metal ion (Zn<sup>2+</sup>). FTIR spectral data indicated that the phytochemical constituents found in the *Andrographis paniculata* extract acts as an efficient stabilizer and reducing agent for the synthesized Zn-Fe<sub>3</sub>O<sub>4</sub> NPs. XRD spectral analysis results indicate that the Zn-Fe<sub>3</sub>O<sub>4</sub> NPs are in the magnetite phase, cubic in structure. The secondary phase is not detected to prove the formation of other zinc-based structures such as simonkolleite and hydroxyzincite. VSM reveals the formation of a superparamagnetic structure with a high saturation magnetization value of 70 emu/g. The major elements present in the EDX spectra are Fe, O and Zn in the Zn-Fe<sub>3</sub>O<sub>4</sub> NPs. The presence of S and C as minor elements was associated with the elemental content of the *Andrographis paniculata* extract. The morphological character of the

obtained sample was investigated by SEM measurements. The antidiabetic activity indicated that the synthesized Zn-Fe<sub>3</sub>O<sub>4</sub> NPs exhibited an improved inhibitory potential against the alpha-amylase enzyme, it also offers a novel approach in nanomedicine for diabetes (type-2) management. The environmentally friendly synthesized Zn-Fe<sub>3</sub>O<sub>4</sub> NPs are suitable in various application fields, especially in biosensing and pharmacological applications.

#### FUNDING

Nil

#### AUTHORS CONTRIBUTIONS

All the authors have contributed equally.

#### CONFLICT OF INTERESTS

The author reports no conflict of interest. The responsible for the writing and content of the article is just the author

#### REFERENCES

- Sebastian A, Nangia A, Prasad MNV. A green synthetic route to phenolics fabricated magnetite nanoparticles from *Coconut husk extract*: implications to treat metal-contaminated water and heavy metal stress in *Oryza sativa* L. *J Cleaner Prod* 2018;174:355–66.
- Harrison RJ, Dunin Borkowski RE, Putnis A. Direct imaging of nanoscale magnetic interactions in minerals. *Proc Natl Acad Sci* 2002;99:16556–61.
- Teja AS, Koh PY. Synthesis, properties and applications of magnetic iron oxide nanoparticles. *Prog Cryst Growth Charact Mater* 2009;55:22–45.
- Lin CR, Chu YM, Wang SC. Magnetic properties of magnetite nanoparticles prepared by mechanochemical reaction. *Mater Lett* 2006;60:447–50.
- Song M, Zhang Y, Hu S, Song L, Dong J, Chen Z, *et al.* Influence of morphology and surface exchange reaction on magnetic properties of monodisperse magnetite nanoparticle. *Colloids Surf A* 2012;408:114–21.
- Lv X, Xu J, Jiang G, Tang J, Xu X. Highly active nanoscale zero-valent iron (nZVI)-Fe<sub>3</sub>O<sub>4</sub> nanocomposites for the removal of chromium (VI) from aqueous solutions. *J Colloid Interface Sci* 2012;369:460–9.
- Gorski CA, Scherer MM. Influence of magnetite stoichiometry on Fe(II) uptake and nitrobenzene reduction. *Environ Sci Technol* 2009;43:3675–80.
- Yew YP, Shameli K, Miyake M, Kuwano N, Ahmad Khairudin NB, Bt Mohamad SE, *et al.* Green synthesis of magnetite (Fe<sub>3</sub>O<sub>4</sub>) nanoparticles using seaweed (*Kappaphycus alvarezii*) extract. *Nanoscale Res Lett* 2016;11:1–7.
- Irina Vedernikova, Alla Koval, Alina Fataliyeva. Thermogravimetric and structural studies of zinc-doped magnetite nanoparticles for pharmaceutical applications. *J Chem Pharm Res* 2018;5:109–12.
- Zhang J, Zhang C, Wei G, Li Y, Liang X, Chu W, *et al.* Reduction removal of hexavalent chromium by zinc-substituted magnetite coupled with aqueous Fe(II) at neutral pH value. *J Colloid Interface Sci* 2017;500:20–9.
- Ahmed S, Saifullah, Ahmad M, Swami BL, Ikram S. Green synthesis of silver nanoparticles using *Azadirachta indica* aqueous leaf extract. *J Radiat Res Appl Sci* 2016;9:1–7.
- Aritonang HF, Koleangan H, Wuntu AD. Synthesis of silver nanoparticles using aqueous extract of medicinal plants' (*Impatiens balsamina* and *Lantana camara*) fresh leaves and analysis of antimicrobial activity. *Int J Microbiol* 2019;1–8. DOI:10.1155/2019/8642303
- Jyoti Pandey, Vimal KS, Wasim Raja. Evaluation of phytochemical analysis of *Andrographis paniculata* leaf and stem extract. *World J Pharm Life Sci* 2019;5:180–90.
- Krishnaveni K, Sakthi Athithan AS, Jeyasundari J, Jacob YBA, Renuga D. Biosynthesis and characterization of zinc doped iron oxide nanoparticles from *Petalium murex* and its new avenues in pharmacological applications. *IOSR J Pharm Biol Sci* 2018;13:67–74.
- Yousefi A, Yousefi R, Panahi F, Sarikhani S, Zolghadr AR, Bahaoddini A, *et al.* Novel curcumin-based pyrano [2,3-d]pyrimidine anti-oxidant inhibitors for  $\alpha$ -amylase and  $\alpha$ -glucosidase: implications for their pleiotropic effects against diabetes complications. *Int J Biol Macromol* 2015;78:46–55.
- Nagajothi S, Mekala P, Raja A, Raja MJ, Senthilkumar P. *Andrographis paniculata*: qualitative and quantitative phytochemical analysis. *J Pharmacogn Phytochem* 2018;7:1251–3.
- Chaki SH, Malek TJ, Chaudhary MD, Tailor JP, Deshpande MP. Magnetite Fe<sub>3</sub>O<sub>4</sub> nanoparticles synthesis by wet chemical reduction and their characterization. *Adv Nat Sci Nanosci Nanotechnol* 2015;6:035009.
- Mohanraj K, Sivakumar G. Synthesis of  $\gamma$ -Fe<sub>2</sub>O<sub>3</sub>, Fe<sub>3</sub>O<sub>4</sub> and copper doped Fe<sub>3</sub>O<sub>4</sub> nanoparticles by sonochemical method. *Sains Malays* 2017;46:1935–42.
- Sutriyo S, Iswandana R, Ivariani FM. Synthesis and stability of resveratrol-gold nanoparticle-polyethylene glycol-folic acid conjugates. *Int J Appl Pharm* 2020;12:237–41.
- Saitawadekar A, Kakde UB. Green synthesis of copper nanoparticles using *aspergillus flavus*. *J Crit Rev* 2020;7:1083–90.
- Ercuta A, Chirita M. Highly crystalline porous magnetite and vacancy-ordered maghemite microcrystals of rhombohedral habit *J Cryst Growth* 2013;380:182–6.
- Suresh J, Pradheesh G, Alexramani V, Sundrarajan M, Hong SI. Green synthesis and characterization of zinc oxide nanoparticle using insulin plant (*Costus pictus* D. Don) and investigation of its antimicrobial as well as anticancer activities. *Adv Nat Sci Nanosci Nanotechnol* 2018;9:015008.
- Jouyandeh M, Ali JA, Aghazadeh M, Formela K, Saeb MR, Ranjbar Z, *et al.* Curing epoxy with electrochemically synthesized Zn-Fe<sub>3</sub>O<sub>4</sub> magnetic nanoparticles. *Prog Org Coat* 2019;136:105246.
- Mahdavi M, Namvar F, Ahmad M, Mohamad R. Green biosynthesis and characterization of magnetic iron oxide (Fe<sub>3</sub>O<sub>4</sub>) nanoparticles using seaweed (*Sargassum muticum*) aqueous extract. *Mol* 2013;18:5954–64.
- Maboudi SA, Shojaosadati SA, Arpanaei A. Synthesis and characterization of multilayered nano-bio hybrid magnetic particles for biomedical applications. *Mater Des* 2017;115:317–24.
- Saratale RG, Shin HS, Kumar G, Benelli G, Kim DS, Saratale GD. Exploiting antidiabetic activity of silver nanoparticles synthesized using *Punica granatum* leaves and anticancer potential against human liver cancer cells (HepG2). *Artif Cells Nanomed Biotechnol* 2017;46:211–22.